Interstitial positions of tin ions in alpha-(FerichSn)(2)O-3 solid solutions prepared by mechanical alloying

Jiang, Jianzhong; Lin, Rong; Nielsen, Kurt; Mørup, Steen; Rickerby, D.G.; Clasen, R.

Published in:
Physical Review B Condensed Matter

Link to article, DOI:
10.1103/PhysRevB.55.14830

Publication date:
1997

Document Version
Publisher's PDF, also known as Version of record

Interstitial positions of tin ions in α-$(Fe_{rich}Sn)_2O_3$ solid solutions prepared by mechanical alloying

J. Z. Jiang* and R. Lin
Department of Physics, Building 307, Technical University of Denmark, DK-2800 Lyngby, Denmark

K. Nielsen
Department of Chemistry, Building 207, Technical University of Denmark, DK-2800 Lyngby, Denmark

S. Mørup
Department of Physics, Building 307, Technical University of Denmark, DK-2800 Lyngby, Denmark

D. G. Rickerby
Institute for Advanced Materials, European Commission, Joint Research Centre, 21020 Ispra (VA), Italy

R. Clasen
INM Institut für Neue Materialien, D-66123 Saarbrücken, Germany
(Received 17 December 1996)

The microstructure of samples of 94, 85, and 71 mol % α-Fe_2O_3-SnO_2, prepared by mechanical alloying, has been studied by x-ray diffraction with Rietveld structure refinements. On the basis of the structure refinements to the whole x-ray diffraction patterns for the four as-milled samples, it is found that tin ions do not substitute iron ions in the solid solution, although this model is generally assumed in the literature. The Sn^{4+} ions occupy the empty octahedral holes in the lattice of the α-Fe_2O_3 phase. [S0163-1829(97)00421-9]

I. INTRODUCTION

Mineral assemblages containing hematite (α-Fe_2O_3) and cassiterite (SnO_2) are of geological and economic importance. Recently, it has been found that α-Fe_2O_3-SnO_2 materials, prepared by a chemical method[1] or mechanical alloying,[2] exhibit a high gas sensitivity to CH_4 and C_2H_5OH gases i.e., the conductivity is significantly altered. These are nanostructured α-Fe_2O_3-SnO_2 solid solutions, whereas the equilibrium mutual solid solubility is negligible at temperatures below 740 K.[3] The microstructure of the α-$Fe_2O_3SnO_2$ solid solutions has been studied by various techniques, such as x-ray diffraction,[1,2,4,5] extended x-ray absorption fine structure[6] (EXAFS), density measurement,[4] optical microscopy,[4] and ^{57}Fe and ^{119}Sn Mössbauer spectroscopy.[1,2,5,7] From the variation of the density,[4] the Mössbauer resonant line broadening,[1,2,7] and the lower Fe-Fe, Sn-Fe, and Fe-O coordination numbers[6] in the (α-$Fe_2O_3)_{rich}$-(SnO_2) solid solutions, it was suggested that anionic and cationic vacancies occur in the α-Fe_2O_3 lattice. In general, it has been assumed that tin ions substitute iron ions in the lattice when tin ions dissolve in α-Fe_2O_3 due to the similar ionic sizes of Fe^{3+} and Sn^{4+}.[1,2,4–11] To the best of our knowledge, no experimental evidence has been reported to examine whether or not the substitution model is valid in this system. In x-ray diffraction studies[1,2] of α-Fe_2O_3-SnO_2 solid solutions prepared by the chemical method or mechanical alloying, some diffraction peak intensities are observed to be dependent on the tin content, and this has not yet been completely understood. The origin of these aspects is the subject of this paper, which will also be of relevance for the α-Fe_2O_3-MO_2 (M=metal element) systems. Four α-$Fe_{rich}Sn_2O_3$ solid solutions prepared by mechanical alloying have been investigated by x-ray diffraction with Rietveld structure refinements. On the basis of structure refinements of these samples, it was found that the substitution model seems to be unable to describe the experimental data. Using a model in which an interstitial position for the dissolved tin ions in α-Fe_2O_3 is proposed, the whole x-ray diffraction patterns for the four samples can be well fitted. It is found that anionic and cationic vacancies are formed. This verifies the suggestion made in earlier studies.[1,2,4,6]

II. EXPERIMENT

Samples of α-Fe_2O_3-SnO_2 were prepared by mixing powders of hematite (α-Fe_2O_3) (99.9% purity, particle size $\approx$10 μm and cassiterite (SnO_2) (99.9% purity, particle size $\approx$10 μm) with three nominal compositions of 94, 85, and 71 mol % α-Fe_2O_3. The milling was carried out in an open container (i.e., the valves on the lid were open during milling) using a planetary ball mill (Fritsch Pulverisette 5), with tungsten carbide (WC) vials and balls.[12] Thus air was constantly available to the oxide powders during milling. The milling intensity was 200 rotations per minute, and a ball-to-powder weight ratio of 20:1 was chosen. The milling time for the first three samples of 94, 85, and 71 mol % α-Fe_2O_3 was 110 h (marked *a* hereafter), and the fourth sample with 71 mol % α-Fe_2O_3 was milled for 151 h (marked *b* hereafter). The compositions of the samples were examined by scanning electron microscopy with an energy-dispersive x-ray analysis facility. It was found that the tungsten contamination originating from the abrasion of the vials

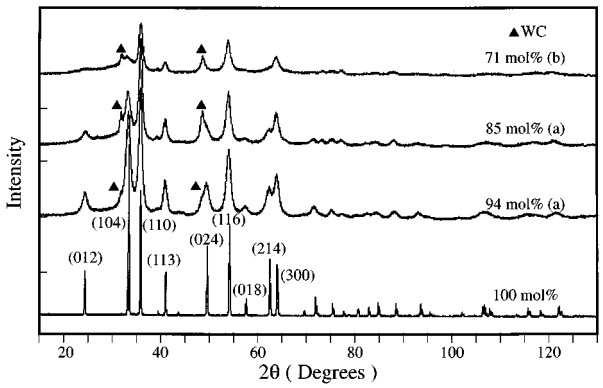

FIG. 1. X-ray powder diffraction patterns for the three as-milled 94, 85, and 71 mol % α-Fe_2O_3-SnO_2 samples with milling times of 110 h (a) and 151 h (b), together with pure unprocessed α-Fe_2O_3.

and balls was less than 2 and 3 at. % for the samples milled for 110 and 151 h, respectively. The samples have been characterized by several experimental techniques: x-ray diffraction, transmission electron microscopy (TEM) and ^{57}Fe and ^{119}Sn Mössbauer spectroscopy. Preliminary results on the alloying process for the 94 mol % α-Fe_2O_3-SnO_2 samples have been published.[7] The x-ray diffraction data were collected in Bragg-Brentano scattering geometry with a Philips PW1820/3711 diffractometer using Cu $K\alpha$ radiation. The data were collected in the 2θ range of 15°–130° with a step length of 0.02° and a counting time of 35 s per step. A graphite monochromator and an automatic divergence slit were used. Normally, using a diffractometer, the surface area exposed to the radiation at small angles is larger than that at large angles. This leads to a systematic error. However, by the application of an automatic divergence slit, the surface area exposed to the radiation is maintained constant during the whole scan and so the systematic error can be limited. The Rietveld refinement program[13] employed pseudo-Voigt functions limited to nine half widths, asymmetry corrections, a Lorentzian component $\gamma = \gamma_1 + \gamma_2 (2\theta)$ and full width at half maximum (FWHM) defined as $(U \tan^2\theta + V \tan\theta + W)^{1/2}$. Here γ_1, γ_2, U, V, and W are fitting parameters. Due to the small grain size in the milled samples, the Bragg peak widths were broadened. Furthermore, the structure in grain boundaries was assumed as an amorphous like structure, which was modeled as a background by 15 parameters (Chebyshev type I).[14]

III. RESULTS AND DISCUSSION

Figure 1 shows the x-ray diffraction patterns of the milled 94, 85, and 71 mol % α-Fe_2O_3-SnO_2 samples together with that of pure unprocessed α-Fe_2O_3. The average grain sizes for the samples prepared by mechanical alloying obtained from TEM observations are ~10 nm, which are in agreement with that previously determined using the Scherrer method.[7] Due to the small grain size for the milled samples, all diffraction peaks are broadened compared to those for pure unprocessed α-Fe_2O_3. By comparing the patterns for the milled α-Fe_2O_3-SnO_2 samples with that for pure unprocessed α-Fe_2O_3, it is found that the positions of the diffraction peaks for the milled samples (except the peaks for the tungsten carbide phase) are almost the same as the corresponding

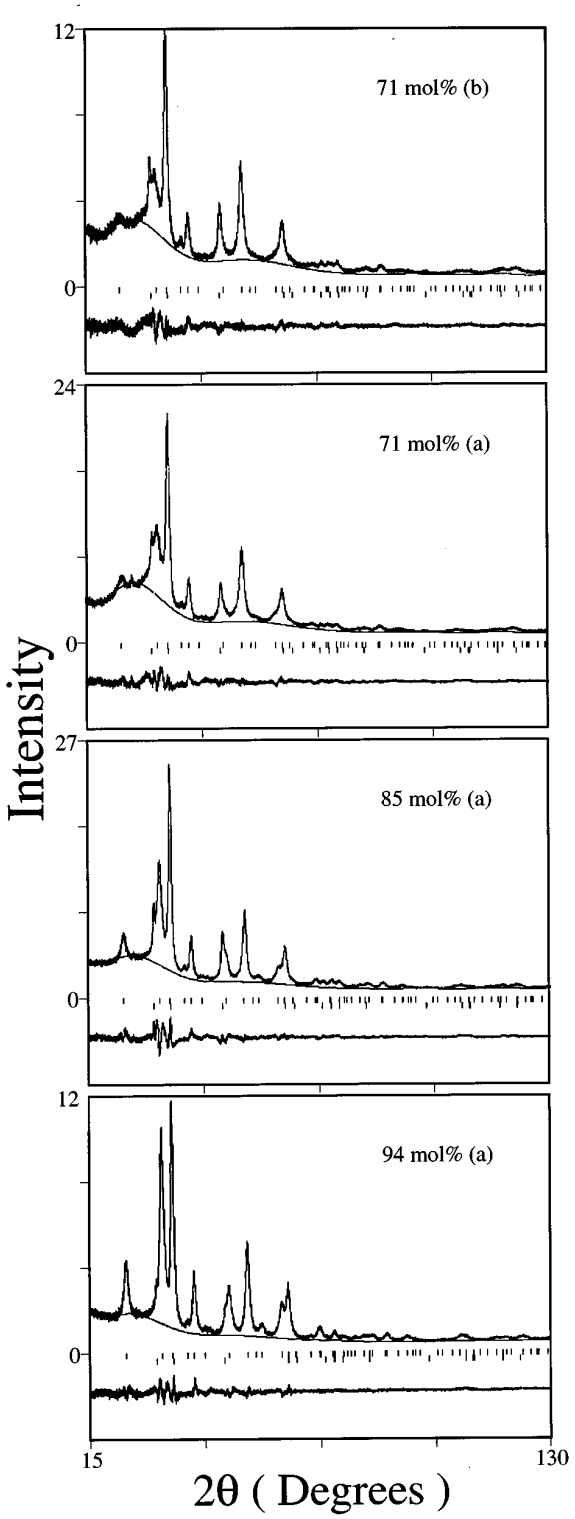

FIG. 2. Rietveld structure refinement profiles of the x-ray diffraction data for the four as-milled 94, 85, and 71 mol % α-Fe_2O_3-SnO_2 samples prepared by mechanical alloying with milling times of 110 h (a) and 151 h (b). The description of the plots is given in the text.

peaks for pure unprocessed α-Fe_2O_3. This implies that the basic structure of the milled samples is still a phase with a structure similar to hematite. However, in all milled samples the diffraction (110) peak is the strongest peak, instead of the (104) peak, which is the strongest one for pure unprocessed

TABLE I. Reliability R factors of the Rietveld structure refinements for the four as-milled 94, 85, and 71 mol % α-Fe_2O_3-SnO_2 samples prepared by mechanical alloying with milling times of 110 h (a) and 151 h (b).

α-Fe_2O_3 (mol %)	R_P (%)[a]	R_{WP} (%)[b]	R_B (hematite) (%)[c]	GOF[d]
94 (a)	4.96	6.32	1.33	2.0
85 (a)	5.79	6.99	1.71	3.7
71 (a)	3.79	4.93	0.83	2.0
71 (b)	4.22	5.52	0.85	1.5

[a]$R_P=\Sigma|y_{obs,i}-y_{calc,i}|/\Sigma y_{obs,i}$, where $y_{obs,i}$ and $y_{calc,i}$ represent the observed and calculated intensities at the ith step, respectively (Ref. 14).

[b]$R_{WP}=[\Sigma w_i(y_{obs,i}-y_{calc,i})^2/\Sigma w_i(y_{obs,i})^2]^{1/2}$ and $w_i=1/y_{obs,i}$ is a weight scheme (Ref. 14).

[c]Bragg peak intensity R-factor $R_B=\Sigma|I_{obs,i}-I_{calc,i}/\Sigma I_{obs,i}$ (Ref. 14).

[d]''Goodness of fit'' GOF$=R_{WP}/R_{expected}$, $R_{expected}=[(N-P)/\Sigma w_i(y_{obs,i})^2]^{1/2}$, where N is the number of observation data and P is the number of fitting parameters (Ref. 14).

α-Fe_2O_3. With increasing tin content in the samples, it is found that intensities of those diffraction peaks with Miller indices (hkl) of $l\neq 3n$, $n=0,1,2,\ldots$, are significantly reduced as compared to pure unprocessed α-Fe_2O_3. A similar result was also reported by Takano *et al.* in chemically synthesized nanostructured α-Fe_2O_3-SnO_2 samples, but no clear explanation to the effect was reported.[1]

In order to clarify the effect, Rietveld structure refinements have been performed for the four milled samples as shown in Fig. 2. The reliability R factors for all Rietveld refinements are listed in Table I. The lattice parameters, ion positions, and ion occupation factors for the milled samples obtained from the Rietveld refinements are listed in Table II and together with the reference data for the pure hematite phase.[15] Before the interstitial model used for the Rietveld structure refinements is introduced, let us consider the structure of pure α-Fe_2O_3. Hematite, α-Fe_2O_3, has a corundum structure with a space group of $R3C$ (No. 167), and one unit cell contains six formula units or ''molecules'' of Fe_2O_3. The hexagonal and rhombohedral structures of hematite are shown in Fig. 3. Its crystal structure is based on the oxygen hexagonal-close-packed lattice. The Fe^{3+} ions with coordinates of $(0,0,z)$, etc., occupy two-thirds of the octahedral holes in successive oxygen layers, and one-third of the octahedral holes with coordinates of (0,0,0), etc., are empty. As mentioned before, it has generally been assumed that tin ions substitute iron ions in the α-Fe_2O_3 lattice due to the similar ionic sizes of Fe^{3+} and Sn^{4+}. From the ^{57}Fe and ^{119}Sn Mössbauer measurements of the four samples,[7,17] it

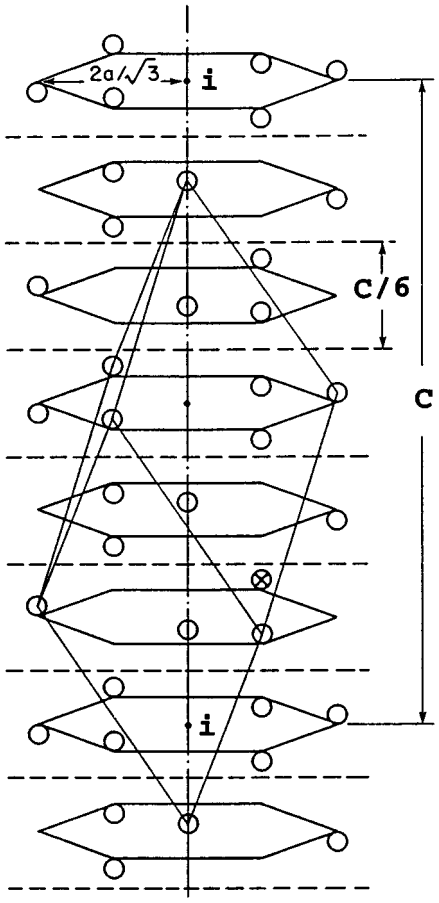

FIG. 3. Atomic arrangements in hematite (Ref. 16). The circles represent Fe^{3+} positions in the hexagonal structure. Note that some iron ions lie above and others below the hexagonal basal planes. The dashed lines indicate the planes in which the O^{2-} ions lie. The outward faces of the rhombohedral cell are also drawn; the circle marked $\times$ represents a corner ion for the inward faces. The origin position is marked with the character i.

TABLE II. Lattice parameters, ion positions, and occupation factors of the hematite like phase obtained by the Rietveld refinement of x-ray powder diffraction patterns for 94, 85, and 71 mol % Fe_2O_3-SnO_2 samples with milling times of 110 h (a) and 151 h (b), together with the reference data for pure unprocessed α-Fe_2O_3 (Ref. 15).

α-Fe_2O_3 (mol %)	Cell parameters		Ion positions[a]		Occupation factor	
	a (Å)	c (Å)	Fe (z)	O (x)	g_{Fe}	g_{Sn}
100	5.038	13.772	0.3553	0.3027	1/3	0
94	5.046(2)	13.817(1)	0.3527(1)	0.3258(6)	0.325(4)	0.004(2)
85	5.058(2)	13.851(2)	0.3504(3)	0.3411(9)	0.308(10)	0.013(5)
71	5.073(4)	13.886(4)	0.3472(3)	0.3333(2)	0.277(10)	0.028(5)
71	5.073(5)	13.892(5)	0.3463(3)	0.3295(9)	0.264(14)	0.035(7)

[a]The iron and oxygen ions have coordinates $(0,0,z)$ and $(x,0,\frac{1}{4})$, respectively.

TABLE III. Calculated values of $|F_H|^2$ for six diffraction peaks with relatively high intensities in the three cases: pure α-Fe_2O_3, the substitution model, and the interstitial model, together with the scattering factors and occupation factors of Fe^{3+}, Sn^{4+}, and O^{2-} ions.

				$\|F_H\|^2$ (a.u.)		
				Pure α-Fe_2O_3 $g_{Fe}=1/3$, $g_O=1/2$	Substitution $g_{Fe}=0.296$, $g_{Sn}=0.028$, $g_O=1/2$	Interstitial $g_{Fe}=0.278$, $g_{Sn}=0.028$, $g_O=0.472$
khl	f_{Fe}[a]	f_O[a]	f_{Sn}[a]			
012	21.326	6.685	43.098	5666	6223	672
104	20.093	6.038	40.953	40314	45494	18383
110	19.705	5.623	40.276	35145	40615	41883
113	18.923	5.176	38.913	6144	6144	5403
024	17.573	4.375	36.558	34598	39045	16609
116	16.848	4.144	35.292	29897	32988	36381

[a]Scattering factors f for all elements are taken from Ref. 18.

was found that no Fe^{2+} and Sn^{2+} ions or metallic tin atoms were present in the milled samples. Hence, in the substitution model, 4/3 Fe^{3+} ions must be removed per Sn^{4+} ion in α-Fe_2O_3 due to charge balance. The first structural model to be refined was the substitution model. This completely failed by leading to negative occupation factors for Sn^{4+} (for example, $g_{Fe}=0.393$ and $g_{Sn}=-0.060$ for the 71 mol % α-Fe_2O_3-SnO_2 sample with a milling time of 151 h). But the difference electron density (observed minus calculated densities) showed an electron density of around (0,0,0), the interstitial position (marked *i* in Fig. 3) along the *c* axis in the hematite structure. Therefore, an interstitial model has been developed to refine the x-ray diffraction patterns for the four samples. In this model, tin ions occupy the empty octahedral holes with coordinates of (0,0,0), etc. The distance between the Sn^{4+} ion position and the two Fe^{3+} nearest neighbors is only ~2 Å. From a physical point of view, it seems impossible that these two cations are so close to each other since the shortest Fe-Fe distance is found to be larger than 2.6 Å in pure α-Fe_2O_3 phase and in the α-Fe_2O_3-SnO_2 solid solutions, listed in Tables IV and V. Consequently, the two Fe^{3+} ions must be removed per Sn^{4+} ion introduced in the structure. Furthermore, to maintain charge balance one O^{2-} ion must be removed per Sn^{4+} ion. This interstitial model has been used in all refinements, by which refinements converged to small *R* values listed in Table I. Attempts to lower the symmetry did not result in any significant improvement of the refinements. In the upper field of each plot in Fig. 2, the experimentally observed pattern is shown. Below that the background is also plotted as a solid line in this field. The difference pattern (observed minus calculated patterns) is plotted in the lower field. In the intermediate field the positions of the possible Bragg reflections are indicated as a series of short vertical bars at different levels corresponding to the different crystalline phases (α-Fe_2O_3 and WC) in the sample. It is found that three phases are present. They are a predominant hematite like phase, a tungsten carbide phase originating from the abrasion of balls and vial, and a broadened background with a major peak at the vicinity of $2\theta=28°$, which may be attributed to an amorphous like phase. ^{57}Fe and ^{119}Sn Mössbauer spectroscopy measurements on the four samples also showed that α-Fe_2O_3-SnO_2 solid solutions are formed during milling.[7,17] The contents of SnO_2 in the solid solutions are found to be about 2.4±2, 7.8±3, 16.8±3, and 21.0±4 mol % for the 94, 85, and 71 mol % α-Fe_2O_3-SnO_2 and the 71 mol % (b) samples, respectively. The dissolution of Sn^{4+} ions in α-Fe_2O_3 results in changes in the lattice parameters of the corundum structure. Both the *a* and *c* axes of the hexagonal cell are elongated. The *a* axis of the hexagonal cell increases with increasing SnO_2 content at a rate of 0.17% per SnO_2 mol %, while the *c* axis increases at a rate of 0.05% per SnO_2 mol %. These values are larger than the data reported in Ref. 1. One possible reason is that the values of the SnO_2 concentration incorporated with α-Fe_2O_3 used in Ref. 1 may be too large because not all SnO_2 in the samples is incorporated in α-Fe_2O_3. The positions of Fe^{3+} ions along the *z* axis and O^{2-} ions along the *x* axis have also been changed by adding Sn^{4+} to α-Fe_2O_3, which could be due to the formation of anionic and cationic vacancies.

To illustrate the peak-intensity dependence on tin content, the values of the square of the absolute value of the structure factor, $|F_H|^2$, for six peaks with relatively higher intensities in three cases of pure α-Fe_2O_3, the substitution model, and the interstitial model are calculated and listed in Table III together with the scattering factors and the occupation factors for Fe^{3+}, O^{2-}, and Sn^{4+} ions, respectively. The integrated intensity of the powder diffraction peaks I_H, where *H* stands for the Miller indices (*hkl*), is proportional to the square of the absolute value of the structure factor, $|F_H|^2$, which is given by,

$$F_H=\sum_j f_j g_j \exp[-2\pi i(hx_j+ky_j+1z_j)] \times \exp\left(-\frac{B_j \sin^2\theta}{\lambda^2}\right),$$

where f_j is the scattering factor for ion j, g_j is the occupation factor of ion j, x_i, y_i, and z_i are the fractional coordinates of the jth ion, and B_j is the temperature factor coefficient. The term $\exp(-B_j \sin^2\theta/\lambda^2)$ results from thermal vibration of ions. For simplicity the thermal vibration effect in the calculation is neglected and only one tin ion in the unit cell is assumed. The qualitative features will still remain when more tin ions are incorporated in the unit cell and the

TABLE IV. Fe-Fe distances (d) and the corresponding average coordination numbers (CN) in the hematite like phase for the 94, 85, and 71 mol % α-Fe_2O_3-SnO_2 samples with milling times of 110 h (a) and 151 h (b), together with the reference data of pure unprocessed α-Fe_2O_3.

α-Fe_2O_3 (mol %)	Fe-Fe (I)		Fe-Fe (II)		Fe-Fe (III)		Fe-Fe (IV)	
	d (Å)	CN[a]	d (Å)	CN	d (Å)	CN	d (Å)	CN
100	2.900	1.00	2.971	3.00	3.364	3.00	3.705	6.00
94	2.838	0.98	2.962	2.94	3.408	2.94	3.714	5.88
85	2.781	0.92	2.958	2.76	3.449	2.76	3.722	5.52
71	2.699	0.83	2.954	2.49	3.507	2.49	3.733	4.98
71	2.673	0.79	2.951	2.28	3.521	2.28	3.734	4.74

[a]CN is defined as $CN=CN_{pure}(g_{Fe}/g_{Fe}^{pure})$ and $g_{Fe}^{pure}=1/3$.

thermal vibration effect is taken into account. In the substitution model, 4/3 Fe^{3+} ions will be removed due to charge balance. In the interstitial model, as mentioned above, two Fe^{3+} ions and one O^{2-} ion will be removed. By comparing the theoretically calculated values of $|F_H|^2$ for the substitution model with those of pure α-Fe_2O_3 (Table III), it is clearly seen that the values of $|F_H|^2$ increase for the substitution model, except for the (113) peak, which is only contributed by the oxygen ions in the lattice. This theoretical prediction is contrary to the experimental x-ray diffraction patterns. On the other hand, for the interstitial model, the intensities of peaks with Miller indices (hkl) of $I \neq 3n$, $n=0,1,2,\ldots$, are dramatically reduced. These results are exactly reflected in the experimental x-ray diffraction patterns observed for the milled samples. Therefore, it can be concluded that the tin substitution model is not suitable to explain the tin ion positions in the α-Fe_2O_3-SnO_2 solid solutions. Based on the refinements, we believe that tin ions occupy the empty octahedral holes when they enter into α-Fe_2O_3 and that anionic and cationic vacancies are formed.

Due to the dissolution of Sn^{4+} ions in α-Fe_2O_3, the local structures around Fe^{3+} ions have been altered. Tables IV and V show the Fe-Fe, Sn-Fe, and Fe-O distances and the corresponding average coordination numbers for the four α-Fe_2O_3-SnO_2 samples and together with the pure unprocessed α-Fe_2O_3. Adding Sn^{4+} ions to α-Fe_2O_3 changes the distances and coordination numbers of Fe-Fe, Sn-Fe, and Fe-O bonds. The first two Fe-Fe nearest distances decrease with increasing the SnO_2 content, while the next two increase. On the other hand, the Sn-Fe nearest-neighbor distance increases with the SnO_2 content in the samples, while the next-nearest-neighbor distance decreases. When more tin ions occupy the empty octahedral holes, more iron ions will be removed from their sites, and hence the average coordination numbers will decrease with increasing SnO_2 content. However, the changes in Fe-O distances are not monotonic for all samples. In the samples with 94 and 85 mol % Fe_2O_3, the Fe-O distance for the first coordination shell is reduced with increasing SnO_2 content, while it increases for the second coordination shell. In the samples with 71 mol % α-Fe_2O_3, the Fe-O distance for the first shell increases, but decreases for the second shell. This is related to the changes in the lattice parameters a and c and the oxygen ion position (x value) in the solid solutions with increasing SnO_2 content. It should be noted that an attempt has been made to compare the data listed in Tables IV and V with those obtained by EXAFS measurements for nanostructured α-Fe_2O_3-SnO_2 samples prepared by the chemical method.[6] It was found that for pure α-Fe_2O_3, the data given by Kanai *et al.*[6] are quite different from the results listed in Tables IV and V, but our results are consistent with the data given by Blake *et al.*[15] Nevertheless, the coordination numbers for the Fe-Fe, Sn-Fe, and Fe-O bonds were reported to decrease when Sn^{4+} ions are dissolved in α-Fe_2O_3,[6] in accordance with the results listed in Tables IV and V. According to the interstitial model

TABLE V. Sn-Fe and Fe-O distances (d) and the corresponding average coordination numbers (CN) in the hematite like phase for the 94, 85, and 71 mol % α-Fe_2O_3-SnO_2 samples with milling times of 110 h (a) and 151 h (b), together with the reference data of pure unprocessed α-Fe_2O_3.

α-Fe_2O_3 (mol %)	Sn-Fe[a]		Sn-Fe (I)		Sn-Fe (II)		Fe-O (I)		Fe-O (II)	
	d (Å)	CN	d (Å)	CN[b]	d (Å)	CN	d (Å)	CN[c]	d (Å)	CN
100	1.933	2.0	2.924	6.0	3.900	6.0	1.954	3.0	2.104	3.0
94			2.926	5.9	3.885	5.9	1.917	2.9	2.172	2.9
85			2.930	5.5	3.874	5.5	1.903	2.8	2.216	2.8
71			2.935	5.0	3.855	5.0	1.947	2.5	2.163	2.5
71			2.934	4.7	3.848	4.7	1.962	2.2	2.141	2.2

[a]When Sn^{4+} ions enter into α-Fe_2O_3, they occupy the (0,0,0) position. Hence the Sn-Fe distances are those from the (0,0,0) position to the surrounding iron ions.

[b]CN is defined as $CN=CN_{pure}(g_{Fe}/g_{Fe}^{pure})$ and $g_{Fe}^{pure}=1/3$.

[c]CN is defined as $CN=CN_{pure}(g_O/g_O^{pure})$, $g_O=0.5-g_{Sn}$ and $g_O^{pure}=1/2$.

proposed here, the chemical formula for the α-Fe_2O_3-SnO_2 solid solutions should be written as $Sn_xFe_{2-2x}O_{3-x}$.

IV. CONCLUSIONS

From the structural refinement analyses of the four as-milled α-Fe_2O_3-SnO_2 samples, it can be concluded that α-Fe_2O_3-SnO_2 solid solutions with high SnO_2 content have been synthesized by mechanical alloying. It was found that the substitution model, as proposed in the literature, cannot be applied to refine the structure of the x-ray diffraction patterns of these solid solutions. An interstitial model, in which the dissolved tin ions occupy empty octahedral holes, has been suggested. The whole x-ray diffraction patterns for the four samples can be fitted well using the model. It is also found that anionic and cationic vacancies have been formed in these solid solutions. This interstitial model will be further examined in the α-Fe_2O_3-MO_2 (M=metal element, e.g., Ti and Zr) systems, which are in progress.

ACKNOWLEDGMENTS

This work was financially supported by the Danish Research Academy and the Danish Technical Research Council.

*Author to whom correspondence should be addressed. Electronic address: jiang@fysik.dtu.dk

[1] M. Takano, Y. Bando, N. Nakanishi, M. Sakai, and H. Okinaka, J. Solid State Chem. **68**, 153 (1987).

[2] J. Z. Jiang, S. W. Lu, Y. X. Zhou, S. Mørup, K. Nielsen, F. W. Poulsen, F. J. Berry, and J. McMannus, Mater. Sci. Forum **235-238**, 941 (1997).

[3] G. H. Moh, Chem. Erde **33**, 243 (1974).

[4] J. Cassedane, An. Acade. Bras. Cienc. **38**, 265 (1966).

[5] S. Musić, S. Popovic, M. Metikos-Hukovic, and V. Gvozdic, J. Mater. Sci. Lett. **10**, 197 (1991).

[6] H. Kanai, H. Mizutani, T. Tanaka, T. Funabiki, S. Yoshida, and M. Tanano, J. Mater. Chem. **2**, 703 (1992).

[7] J. Z. Jiang, R. Lin, S. Mørup, K. Nielsen, F. W. Poulsen, F. J. Berry, and R. Clasen, Phys. Rev. B **55**, 11 (1997).

[8] F. Schneider, K. Melzer, H. Mehner, and G. Dehe, Phys. Status Solidi A **39**, K115 (1977).

[9] P. B. Fabritchnyi, E. V. Lamykin, A. M. Babechkin, and A. N. Nesmeianov, Solid State Commun. **11**, 343 (1972).

[10] E. Realo and S. Reiman, in *Proceedings of the International Conference on Mössbauer Spectroscopy*, Cracow, 1975, edited by A. Z. Hrynkiewicz and J. A. Sawicki (Wykonano w Powielarni Akademii Gorniczo-Hutniczej im S. Staszica, Cracow, 1975), p. 373.

[11] T. Okada, A. Ambe, F. Ambe, and H. Seklzawa, J. Phys. Chem. **82**, 4726 (1982).

[12] J. Z. Jiang, Y. X. Zhou, S. Mørup, and C. B. Koch, Nanostruct. Mater. **7**, 401 (1996).

[13] C. J. Howard and R. J. Hill, Program LHMP1, Australian Atomic Energy Commision Report M112, Lucas Hights Research Laboratory, New South Wales, Australia, 1986.

[14] *The Rietveld Method*, edited by R. A. Young (Oxford University Press, New York, 1993).

[15] R. L. Blake, R. E. Hesserick, T. Zoltai, and L. W. Finger, Am. Mineral. **51**, 123 (1966).

[16] A. H. Morrish, *Canted Antiferromagnetic: Hematite* (World Scientific, Singapore, 1994), p. 19.

[17] J. Z. Jiang *et al.* (unpublished).

[18] *International Tables for X-Ray Crystallography*, edited by C. H. Macgillavry, G. D. Rieck, and K. Lonsdale (The Kynoch Press, Birmingham, England, 1968), Vol. 3.